# COMPATIBILITIES OF $YBa_2Cu_3O_{9-\delta}$ TYPE PHASE IN QUINTENARY SYSTEMS Y—Ba—Cu—O—X (IMPURITY)

P. Karen, O. Braaten, H. Fjellvåg and A. Kjekshus
Department of Chemistry, University of Oslo, Blindern, N-0315 Oslo 3, Norway

Isothermal phase diagrams at various oxygen pressures are investigated by powder diffraction and chemical analytical methods. The components, Y, Ba, Cu, and O, (specifically $O_2$, $O^{2-}$ and $O_2^{2-}$) are treated, together with C (specifically $CO_2$ and $CO_3^{2-}$), alkaline metals, Mg, alkaline earths, Sc, 3-d and 4-f elements. Effects of the substitutions at the structural sites of $YBa_2Cu_3O_{9-\delta}$ on $T_c$ are discussed with respect to changes in crystallochemical characteristics of the substituted phase and to the nature of the substituents.

## 1. INTRODUCTION

Electrical transport properties of the oxidic high-Tc superconductors are significantly affected by the presence of minor amounts of various elements added inadvertently as impurities, e.g., from the chemical environment during manufacturing. $YBa_2Cu_3O_{9-\delta}$ tends to lose its superconductivity upon (partial) substitution of any of the four elemental components. Most of the substituents, and particularly Pr (for Y) [1], La (for Ba) [2,3], Fe, Co, Ni and Zn (for Cu) [4], alter some of the prerequisites of superconductivity, such as mixed valency state in the Cu—O network or a structural distortion of the network [5,6].

Although various pseudo-ternary equilibrium chemical phase diagrams of the Y(O)—Ba(O)—Cu(O) system have been proposed [7-11], no consensus has been reached to date, partly due to inconsistent equilibrium conditions. Even less information is available [12,13] about the phase compatibilities in the appropriate quaternary phase diagram (including oxygen and implying redox relations). Virtually no information exists about any quintenary phase diagrams (including one additional element). Due to the complexity of such systems, also this presentation is limited to more or less close surroundings of the $YBa_2Cu_3O_{9-\delta}$ type phase (123) in the appropriate pseudo-quaternary or pseudo-pseudo-ternary diagrams.

## 2. EXPERIMENTAL

Samples were prepared by liquid mixing in citrate gels using basic copper carbonate, barium carbonate and yttrium oxide. Additional metal oxides were introduced into the gels in a water soluble (complexed) form. The incinerated gels were fired repeatedly in purified oxygen, with intermittent rehomogenizations followed by a 16 h equilibration at 340 °C. Low $O_2$ pressures above the samples were maintained (when neccessary) by means of $Cu_2O/CuO$, $Cu/Cu_2O$ or Ni/NiO getters in closed systems at variable temperatures. The degree of (de)oxidation was determined iodometrically. Gravimetrical analyses by reduction in pure $H_2$ at 1000 °C were also performed. The carbon was determined coulometrically as $CO_2$ released from the sample at 1100 °C in oxygen. The equilibria of the reactions with $O_2$ and $CO_2$ were investigated by a thermogravimetric analysis (TGA). Powder X-ray diffraction data (PXD) were collected using Guinier-Hägg cameras. Powder neutron diffraction data (PND) were collected with a two-axis diffractometer at 8-300 K. Structural parameters were refined according to the Rietveld method. Magnetic susceptibility was measured using a SQUID magnetometer at 4-300 K in a 10-30 G magnetic field. $T_c$ is evaluated as the point with 0.5 % of the remaining Meissner effect upon increasing temperature conditions.

## 3. THE PHASE SYSTEMS

### 3.1. The System Y-Ba-Cu-O

Due to the variable valency of copper, a true quaternary system should be considered, including also redox interphase relations. Although the redox reactions (decompositions) of the particular phases

occur at generally different partial pressures of oxygen, for practical reasons only some isobaric phase diagrams are reported here. As another experiment–related constraint, the corner adjacent to the highly reactive BaO is omitted from consideration in the phase diagrams.

At *high oxygen partial pressures*, $Cu^{III}$ (formally) compounds may be stabilized. $YCuO_3$ and $BaCuO_{2.5}$, are formed under $\sim$ 300 atm $O_2$ pressure and reported [15,16] to be stable up to some 600 °C. At higher temperatures, the highest attainable copper valency decreases. At 910 °C, the ambient pressure phases, *viz.*, $Y_2Cu_2O_5$ and $BaCuO_{2+\nu}$, together with $Y_2BaCuO_5$ (211), are apparently stable even at high oxygen pressures. In principle, the 123 phase is preserved as well [10,17,18]. At such conditions, though, in some reports [19,20], it is proposed to accommodate additional oxygen as peroxygroups. Two other phases occur, which are closely structurally related to 123, *viz.*, $Y_2Ba_4Cu_7O_{\sim 15}$ (247), stable between 7 and 20 atm $O_2$ at 910 °C, and $YBa_2Cu_4O_{\sim 8}$ (124), stable above $\sim$20 atm $O_2$ at 910 °C [21].

For *1 atm $O_2$ pressure*, the phase diagram at 910 °C is shown in Fig. 1A. A portion of the diagram is already above the solidus line, and $YBa_2Cu_3O_{9-\delta}$ melts incongruently at $\sim$ 960 °C [22]. Below 830 °C, the 124 phase is stable also at the 1 atm oxygen pressure, see Fig. 1B. This is connected apparently with the increased stability of $Cu^{II}$ at lower temperatures, which preserves the double–square structural chains of copper and oxygen atoms. At 800 °C, no formation of 123 is observed upon prolonged annealing of 124 (>200 h, and rehomogenizations). Neither the parallel extended annealing of 123 provides indices for decomposition of 123 into the neighbouring phases, *viz.*, 124, 211 and $BaCuO_{2+\nu}$.

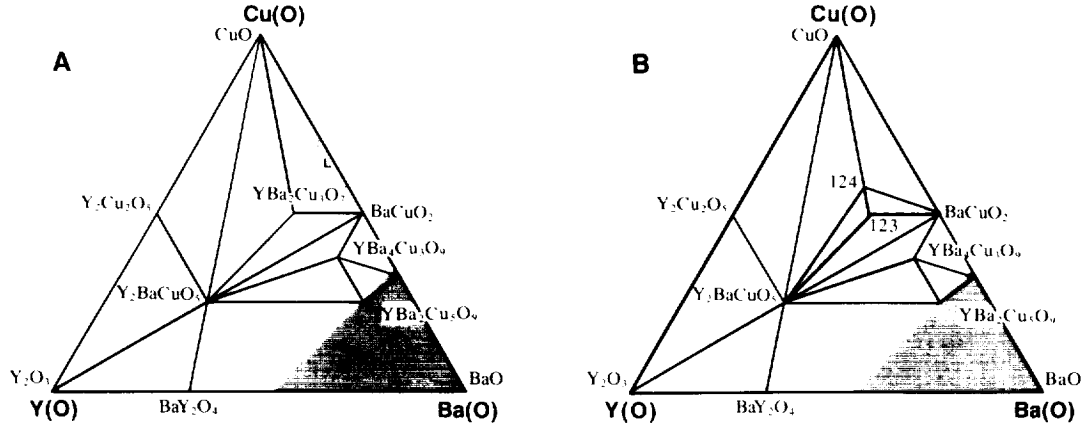


**Figure 1.** Equilibrium phase diagram Y—Ba—Cu—O, projected onto the plane of metallic components for 1 atm oxygen partial pressure at 910 °C (A) and 800 °C (B). BaO–rich phases omitted.

*Low oxygen partial pressures* at high temperatures lead to decomposition of the copper–rich, $Cu^{II}$ containing phases, particularly those which cannot accommodate substantial amounts of $Cu^{I}$ in their structures, like 124 or $BaCuO_{2+\nu}$. The 124 phase becomes unstable even at temperatures below 830 °C, and its rapid decomposition into CuO and 123 is observed at, e.g., 800 °C for $\sim 1.3 \cdot 10^{-3}$ atm $O_2$, above $Cu_2O/CuO$. In addition, some of the Ba–rich quaternary oxides become less stable at these conditions, e.g., $YBa_4Cu_3O_{\sim 8}$ (143) decomposes into $BaCuO_{2+\nu}$, $Y_2BaCuO_5$ and a more Ba–rich quaternary oxide. The 123 phase decomposes into the $Cu^{II}$ containing, however, Cu–poor and very stable phase $Y_2BaCuO_5$, and into $BaCu_2O_2$ and a Ba–rich quaternary oxide, e.g., at 850 °C and $4 \cdot 10^{-4}$ atm $O_2$ [12].

At even lower oxygen pressures, the $Y_2Cu_2O_5$ phase is also reduced, *viz.*, into $YCuO_2$. If the oxygen pressure is further lowered, e.g., to $2.4 \cdot 10^{-14}$ atm, above the Ni/NiO system at 820 °C, all the Cu containing phases decompose into metallic Cu and oxides from the pseudo–binary section

Y—Ba—O, see Fig. 2.

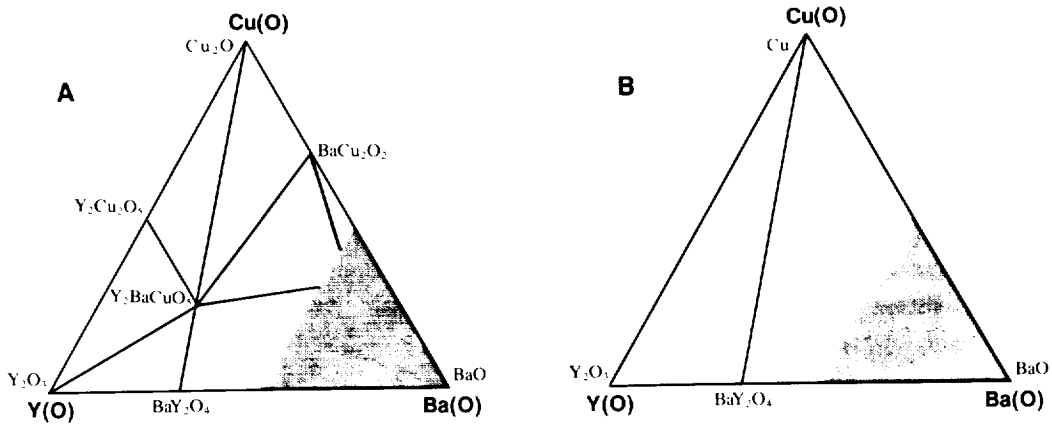


**Figure 2.** Equilibrium phase diagram Y—Ba—Cu—O, projected onto the plane of metallic components at 820 °C for low oxygen partial pressures, *viz.*, $2.5 \cdot 10^{-9}$ atm above $Cu/Cu_2O$ (A) and $2.4 \cdot 10^{-14}$ atm above Ni/NiO (B). BaO-rich phases omitted.

### 3.2. The Y—Ba—Cu—O—□ System

With an exception of the $Y_2BaCuO_5$ phase, all the other quaternary phases contain mixed-valent Cu. This is related to the presence of oxygen vacancies in their structures, and the phases therefore have a homogeneity range with respect to the oxygen content, see Table I.

**Table I.** Oxygen content, unit cell parameters and volume for some oxidized and reduced (the latter above $Cu/Cu_2O$ or $Cu_2O/CuO$), mixed-valent Y—Ba—Cu—O phases.

| formula | t (°C) | $p_{O_2}$ (atm) | $x$ | $a$ (Å) | $b$ (Å) | $c$ (Å) | V (Å$^3$) |
|---|---|---|---|---|---|---|---|
| $YBa_2Cu_4O_x$ | 340 | 1.0 | 7.99(2) | 3.8427(10) | 3.8704(6) | 27.250(5) | 405.3(1) |
| $YBa_2Cu_3O_x$ | 340 | 1.0 | 6.96(2) | 3.8187(3) | 3.8859(3) | 11.6795(11) | 173.32(2) |
| | 800 | $> 10^{-3}$ | 6.18(3) | 3.8599(2) | — | 11.8061(9) | 175.90(2) |
| | 800 | $> 10^{-9}$ | 6.00(5) | 3.8583(1) | — | 11.8253(8) | 176.03(2) |
| $BaCuO_x$ | 340 | 1.0 | 2.09(1) | 18.303(6) | — | — | 6132(6) |
| | 800 | $> 10^{-3}$ | 2.00(2) | 18.293(4) | — | — | 6121(4) |
| | 800 | $> 10^{-9}$ | 1.98(2) | 18.288(4) | — | — | 6116(4) |
| $YBa_4Cu_3O_x$ | 340 | 1.0 | 9.21(2) | 8.102(2) | — | — | 531.8(4) |

Formally, the deoxidation process may be treated as a pseudochemical equilibrium between the gas phase and the vacancies in the solid. Unlike the true chemical equilibrium, the composition of the individual solid phase also varies, and the equilibrium should be expressed in a three dimensional space. In Fig 3, such equilibrium is exemplified [14] by $YBa_2Cu_3O_{9-\delta}$.

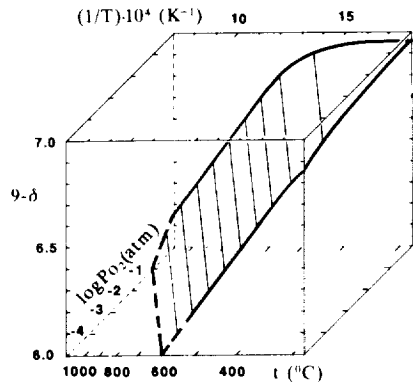


**Figure 3.** Pseudochemical equilibrium diagram between $YBa_2Cu_3O_{9-\delta}$ and oxygen as a function of partial pressure ($p_{O_2}$), temperature (T, t) and composition ($9 - \delta$) as obtained by TGA.

### 3.3. The Y—Ba—Cu—O—C System

This system is of considerable importance, since carbon (particularly $CO_2$) is a component of various chemical environments and specifically, some common oxide-preparation routes involve carbon compounds which ultimately become carbonates. Specifically, the Y(O)—Ba(O)—Cu(O)—$CO_2$ system and a high temperature reaction of $CO_2$ with $YBa_2Cu_3O_{9-\delta}$ are shown here as important examples.

Ba forms an extremely stable carbonate, due to its high electropositivity and the relatively large ionic size. It is, therefore, not surprising that carbonate anions may be stabilized as oxidecarbonates in the Ba rich regions of the oxidic phase systems. Considering the *Y(O)—Ba(O)—Cu(O)—$CO_2$ system*, the oxidecarbonate stability may prove to be particularly significant if barium carbonate appears as a starting material or as a reaction intermediate. Examples of such phase diagrams are shown in Fig. 4.

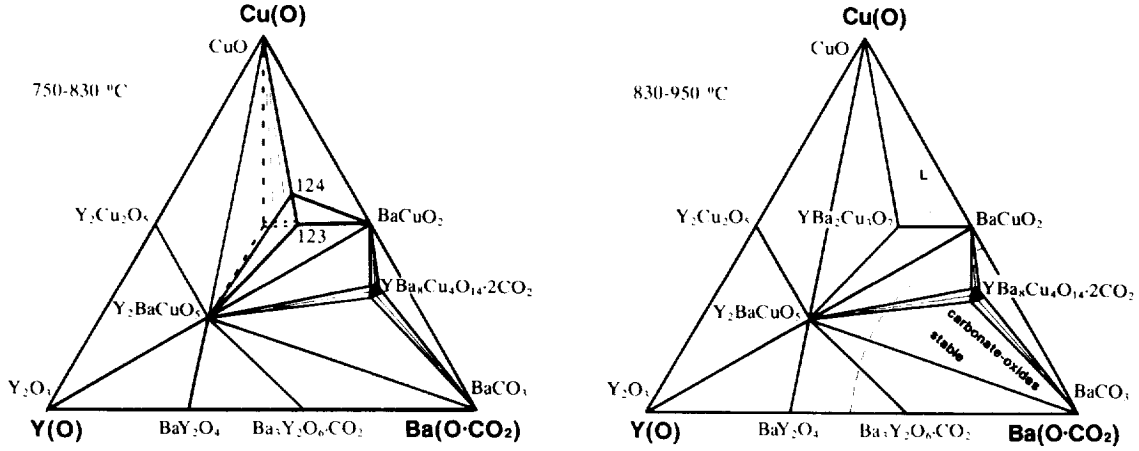


**Figure 4.** Phase diagrams of the Y(O)—Ba(O)—Cu(O)—$CO_2$ system at various temperatures as seen after equilibrium firing of carbonate-containing starting materials in 1 atm $O_2$ ($\leq$ 5 ppm $CO_2$). Metastable phases are marked by dashed lines. An above-solidus region is marked by dotted lines for $\sim$ 950 °C.

Oxidic materials may be obtained from carbonate precursors in $O_2$ at relatively low temperatures, say above 750 °C, if a liquid-mixing technique is used and the composition of the oxide phase is not too rich in BaO. Thus, between $\sim$ 750 and 830 °C, the 123 phase is still formed, however, with unusual structural characteristics. Its crystal structure is tetragonal with $a$ = 3.8738(3) Å and $c$ = 11.612(4) Å, but the diffraction pattern shows apparent signs of structural disorder. The enhanced unit cell parameter $a$ and the contracted parameter $c$ may indicate substitution by carbonate or peroxyanions into the Cu—O chains. The carbon analyses and the $H_2$-reduction gravimetrical analyses of independent samples indicate a presence of 0.1 to 0.2 $CO_2$ per formula unit, while no enhanced oxygen content is indicated by iodometry. The possibility of a corresponding presence of up to $\sim$ 7 wt.% of $BaCO_3$ in the samples is not substantiated by PXD. For parallel samples of 124, less than 0.02(1) $CO_2$ (per 124) is found. The oxidecarbonate stabilization up to an approximate formula $YBa_2Cu_3O_{6.8}(CO_3)_{0.2}$ is therefore feasible. It is remarkable that an extended ability of the Ba-site to accommodate smaller substituents is shown by this phase. Actually, up to approximately 1/3 of Ba may be statistically replaced by Y. During repeated firings, this substituted phase decomposes much faster than the parent (oxidecarbonate) phase, indicating that the random Y/Ba distribution is a remnant of the atomic-level mixing in the citrate precursor, rather than representing any real thermodynamic stability.

More defined oxidecarbonates are formed in the region closer to the Ba corner. In the literature, they are often misinterpreted as true oxides. Up to 950 °C, a 184 phase is formed,

$Y_{1+x}Ba_8Cu_{4+z}(CO_3)_2O_{10+\eta}$, having both cationic and anionic vacant, perovskite based structure, the rough features of which are outlined in [23,24]. Its range of homogeneity with respect to the metal content extends to $x = 0.3$ or $z = 0.5$. The content of the anionic component may be varied in a similar way as with the 123 compound, i.e., in a gas–vacancy equilibrium. The oxygen saturated 184 phase has $\eta = 2.08(2)$. Deoxidation at 800 °C above the $Cu/Cu_2O$ system leads to $\eta = 1.05(2)$. If the additional metal atoms ($x > 0, z > 0$) are introduced into the vacant cationic sites, $\eta$ increases proportionally. None of the purely oxidic phases reported by De Leeuw et al. [25] in the vicinity of the 184 composition are formed in oxygen (< 5 ppm $CO_2$) from carbonaceous starting materials below 950 °C. Of these phases, 143 and 152 are readily formed at 1000 °C, whereas formation of the other two reported phases, 385 and $Ba_2CuO_3$, was not observed after 4 times firing in oxygen for 20 h. In the subsolidus region (< 1000°C), the 184 phase starts to decompose slowly and incompletely above 950 °C, under formation of phases having distorted and disordered, 143 and 152–related structures, besides yet unidentified intermediates.

Another oxidecarbonate is formed in the Y—Ba—O pseudo–binary section. The phase earlier named $Y_2Ba_2O_5$, which always was found in multi–phase mixtures, was shown [25] to be an oxidecarbonate. Its actual composition is $Y_2Ba_3O_6 \cdot \sim 0.6CO_2$, and it has a tetragonal crystal structure (currently being solved from PXD and PND data) with $a = 4.3861(5)$ Å and $c = 23.719(4)$ Å which is reminiscent of that of $Sr_3Ti_2O_7$ [26]. The oxidecarbonate decomposes abruptly at 980 °C in "pure" oxygen (<5 ppm $CO_2$). Another apparent analogue of the Sr, Ti oxides [26] is $Y_3Ba_4O_7 \cdot CO_2$ which is formed above 1000 °C [25]. Obviously, an array of oxidecarbonates exists here with increasing BaO content and increasing decomposition temperature.

If the $CO_2$ content in the atmosphere during firing is increased, both the oxidecarbonates and the pure oxides are subject to a more complete reaction with $CO_2$. This carbonatization transfers all the present barium into $BaCO_3$. The other reaction products may be variable, as exemplified by the *reaction of $YBa_2Cu_3O_{9-\delta}$ with $CO_2$* in Fig. 5. Namely, below 730 °C, only binary oxides occur in the reaction products besides barium carbonate, whereas $Y_2Cu_2O_5$ is formed [14] at higher temperatures.

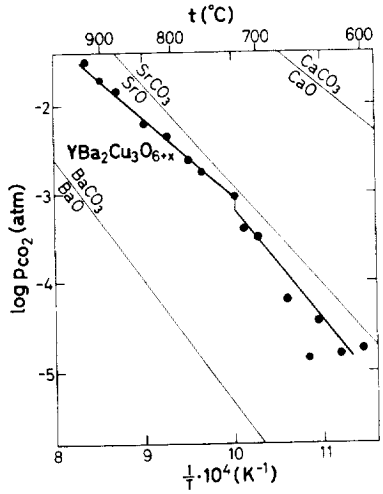


**Figure 5.** $YBa_2Cu_3O_{9-\delta}$ stability with respect to carbonatization in $O_2/CO_2$ atmospheres at ambient pressure. The equilibrium state is tentatively indicated by the solid line and the shaded strip. Thinner lines depict calculated data for alkaline earths.

The equilibrium in Fig. 5 illustrates that the average basicity of the 123 oxide at high temperatures may be compared with that of SrO. For any judgement about the stability of 123 in a reaction atmosphere, it may be of importance that the reaction of 123 with a dry, $CO_2$–containing gas is not effectively stopped by the kinetics until a temperature below 400 °C is reached.

### 3.4. The Systems RE—Y—Ba—Cu—O, RE = Rare Earth Element

Introduction of another RE into the Y—Ba—Cu—O system leads in many cases to formation of a solid solution due to the chemical similarity of the rare earths. Ce, Tb and pairs of the dimensionally very different RE's are examples of breaking this rule. Though some of these phases have very interesting superconducting properties, they fall outside the titled scope of this paper.

Many of the RE elements may, at least partially, be accommodated at the Y–site and some even at the Ba–site of $YBa_2Cu_3O_{9-\delta}$ as well as of neighbouring phases in the phase diagram. In

$YBa_2Cu_3O_{9-\delta}$, yttrium may be fully replaced by the rare earths Yb-to-Dy and Gd, Eu and Sm. According to equilibrium samples fired at 910 °C, and oxygen saturated at 340 °C, Lu and Tb replace Y up to 1/3. For Nd, Pr and La, an occupational equilibrium between the Y and Ba sites exists, which means that the Ba site may accommodate large rare earths. For the smallest of these, Nd, the equilibrium favours occupation of the Y-site, whereas the Ba-site is preferred in the case of La. No substitution solely for Y may be reached using Nd and larger rare earths, neither may any substitution solely for Ba be obtained for Pr and smaller rare earths. If the former is attempted, the $BaCuO_{2+\nu}$ impurity phase binds the simultaneously replaced Ba. If the latter is attempted, an $Y_2BaCuO_5$-type phase binds the simultaneously replaced Y and emerges together with CuO. Only La is large enough not to attack the Y-site unless it is present at the Ba-site in a concentration higher than 35%. In which case, Y is substituted by La as well and emerges as $Y_2Cu_2O_5$. In Fig. 6., these situations are shown in tetrahedral diagrams. Cerium does neither substitute Y nor Ba by more than a few %. The excess Ce is bound into both $BaCeO_3$ and $(Ba,Ce,Y)_2CuO_4$ ($T^*$-type [27]) phases, emerging together with $BaCuO_2$ as impurities to 123.

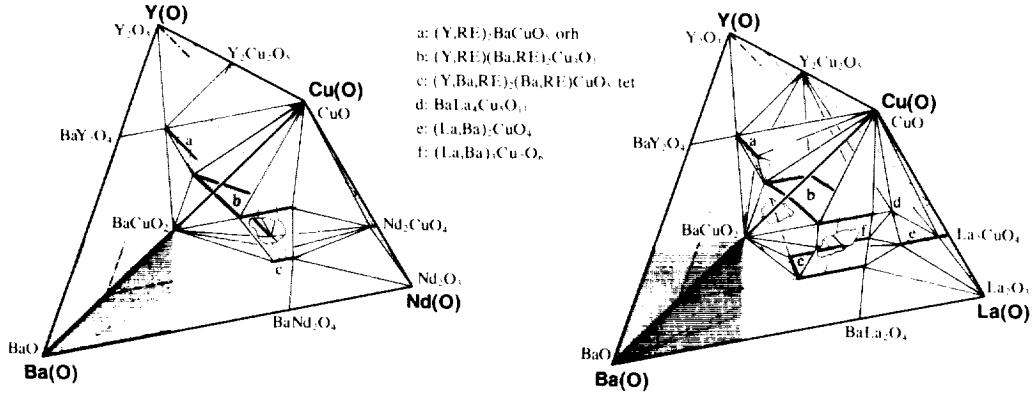


**Figure 6.** Pseudo-quaternary tetrahedral phase diagrams of RE—Y—Ba—Cu—O system for RE = Nd and La, for samples fired at 910°C and oxygen saturated at 340°C. Floors at 25 and 50 pseudoatom-% Cu are drawn as nontransparent and marked by broken line. The $(Y,RE)(Ba,RE)_2Cu_3O_{9-\delta}$ solid solution regions in the pseudo-pseudo-ternary cut are dotted. BaO-rich phases omitted (dashed region).

As may be apparent in Fig. 6, the $Y_2BaCuO_5$ phase has a higher accommodative ability for smaller RE's than does the 123 phase. On the other hand, already for Nd and larger RE's, another structure type is adopted for the 211 phase. Extended regions of solid solubility are found in the pseudo-binary systems between phases $Y_2BaCuO_5$ and $Nd_2BaCuO_5$ type e.g., the mutual solid solubility Nd/Y is respectively 85 and 5 mole-%. The corresponding values for the La/Y pair are respectively ~30 and ~10 mole-%. The $Nd_2BaCuO_5$ type structure may moreover accommodate some Ba at the RE-sites, *viz.*, 0-15 % for RE = Nd and 4-65 % for RE = Nd and La.

A substitution of Ba by the larger RE's (Nd to La) in the $BaCuO_{2+\nu}$ phase is obviously possible as indicated by a decrease in its unit cell volume in some investigated systems. However, no exact data are available and the solid solutions are not shown in Fig. 6.

Specifically for La, a close neighbouring phase occurs to the $(Y,La)(Ba,La)_2Cu_3O_{9-\delta}$ frontier of the solid solution area in the phase diagram. This phase, $(La,Ba)_3Cu_2O_x$, has a region of homogeneity around the La/Ba ratio 1/1. Probably, the phase has also a small solid solubility region towards Y.

### 3.5. The Systems Ca/Sr—Y—Ba—Cu—O

Due to considerable differences in size between the Ca, Sr and Ba ions, different structures are frequently adopted with the same nominal composition. For the same reason, only limited regions

of solid Sr/Ba miscibility are observed in the particular phases here under consideration. No indications were found for any Ca/Ba miscibility and the Sr/Y substitution limit is close to zero. On the other hand, by size considerations, the aliovalent Ca/Y substitution is feasible. However, the process only occurs in oxygen-defect phases, like $YBa_2Cu_3O_{9-\delta}$, where Ca may substitute for Y up to 25 %. The Sr substitution in $YBa_2Cu_3O_{9-\delta}$ is exemplified here more particularly. Replacement up to 35 % is reached. Above this limit, $Y_2BaCuO_5$ and $Sr_{14}Cu_{24}O_{41}$ [29] emerge as impurity phases. If substitution of Sr for Y is attempted, virtually no replacement, $(4 \pm 4)\%$, is achieved; a portion of Ba is substituted instead, and $BaCuO_2$ appears as impurity. This situation is shown in Fig. 7.

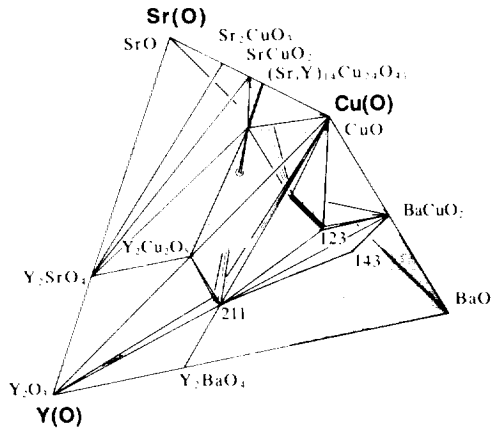


**Figure 7.** Pseudo-quaternary tetrahedral phase diagram of the Sr—Y—Ba—Cu—O system, for samples fired at 910°C and oxygen saturated at 340°C. A non-transparent floor at 50 pseudoatom-% Cu is marked by a broken line. BaO-rich phases omitted (dashed region).

### 3.6. Substitution for Ba and Y in $YBa_2Cu_3O_{9-\delta}$ by Alkali Metals

Contrary to some reports, a rather limited substitution by alkali metals into $YBa_2Cu_3O_{9-\delta}$ is found, although various precautions were taken to prevent evaporation of the alkali metal peroxides which are readily formed in the system, *viz.* by using closed system, reducing atmosphere or vapour saturation from additional peroxide. At 850 °C, no more than ~ 8 % of Ba is replaced by Na, with possibly up to 4 % of Y being replaced simultaneously. No substitution of Ba with elements similar in size, K-to-Cs, was accomplished for levels above 10 %.

### 3.7. Substitution for Cu in $YBa_2Cu_3O_{9-\delta}$ by Li, Mg and 3-d Elements

The affinity of these substituents for the Cu-sites follows the common trends of chemical similarity, as defined by, e.g., electronic configuration, coordination and ionic size. The substitutions preserve the formal high oxidation state of Cu, and the substituents themselves adopt high valency states, *e.g.*, $Fe^{III}$, $Co^{III}$, $Ni^{>II}$, which in turn is reflected in the oxygen content per formula unit, $9 - \delta$. The compositional limits, obtained by mass-balances from PXD quantitative analyses, are listed in Table II, together with (identified) phases in equilibrium at the substitution limit [4].

**Table II.** Qualitative phase composition at the limits of solid solubility for Li, Mg and first row transition metal (M) substitution in $YBa_2(Cu_{1-z}M_z)_3O_{9-\delta}$ for firings at 910 °C and oxidation at 340 °C.

| M | $Y_2BaCuO_5$ | $BaCuO_{2+\nu}$ | other observed phases | $z_{max.}$ | $(9-\delta)_{z_{max}}$ |
|---|---|---|---|---|---|
| Li | + | + | $BaCO_3$, $Li_2CO_3$ | 0.04(1) | 6.90 |
| Mg | + | + | MgO | 0.04(1) | 6.88 |
| Sc | + | – | $BaSc_2O_4$ | 0.01(1) | 6.96 |
| Ti | + | – | [a] barium titanates | 0.00(2) | 6.96 |
| V | + | – | $Ba_3V_2O_8$ | 0.00(4) | 6.96 |
| Cr | + | – | $BaCrO_4$ | 0.02(1) | 6.96 |
| Mn | + | – | $Ba_3Mn_2O_8$ | 0.00(3) | 6.96 |
| Fe | – | +[b] | [c] $BaFeO_3$ + ? | 0.22(1) | 7.17 |
| Co | – | – | ? | 0.30(5) | 7.23 |
| Ni | +[d] | +[d] | NiO | 0.08(1) | 6.98 |
| Zn | +[d] | +[d] | – | 0.09(1) | 6.90 |

[a] $Ba_2TiO_3$, $BaTi_2O_5$, $BaTi_4O_9$. [b] Fe/Cu substitution occurs; $Ba(Cu_{1/3}Fe_{2/3})O_{2+\nu}$, from $a$ = 1842.4(4) pm by molar volume difference, $\mathcal{V}_{FeO_x} - \mathcal{V}_{CuO_x}$, [c] $a$ = 408.4(3) pm. [d] Ni/Cu, Zn/Cu substitution.

## 4. SUPERCONDUCTING PROPERTIES OF SUBSTITUTED $YBa_2Cu_3O_{9-\delta}$

### 4.1. Y–substituted $YBa_2Cu_3O_{9-\delta}$

Substitutions for Y which do not change the charge balance in the compound, do not affect the superconducting properties. This is valid particularly for substitutions by trivalent rare earths [30] of the type $(Y_{1-x}M_x)Ba_2Cu_3O_{9-\delta}$. However, a decrease in $T_c$, $(\partial T_c/\partial x)_{x\to 0} = -200$ K, is observed if Pr is partially introduced into the Y-site (and necessarily into a small portion of Ba simultaneously, see 3.4.). This may be explained by an electron injection of the Cu—O net from the *mixed valent* $Pr^{>III}$ which generally may act as a sort of charge buffer during the pairing process. Remarkably, Tb, if substituted for Y, behaves in conformity with the valency III and no decrease in $T_c$ is observed. If a lower valent element is substituted for Y, like Ca, the oxygen content is decreased and a decrease in $T_c$ is observed, with derivative $(\partial T_c/\partial x) = -50$ K.

### 4.2. Ba–substituted $YBa_2Cu_3O_{9-\delta}$

Of the few elements which may substitute solely according to the $Y(Ba_{1-y}M_y)_2Cu_3O_{9-\delta}$ formula, i.e., without simultaneously entering the Y-site, both La and Sr cause a decrease in $T_c$, with $(\Delta T_c/\Delta y)_{y=0,0.2} \approx -250$ K for M = La (non-linear) and $(\partial T_c/\partial y)_{y\in 0,0.3} = -20(2)$ K for M = Sr, in oxygen saturated samples [6,29,30]. The results for La substituted samples [6] are shown in Fig 8.

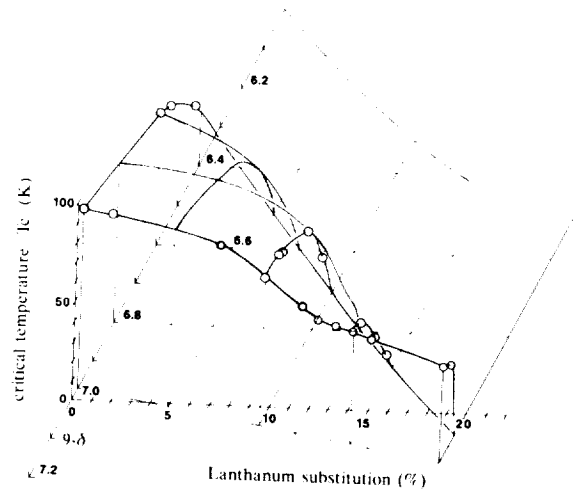


**Figure 8.** $T_c$ (in K) for $Y(Ba_{1-y}La_y)_2Cu_3O_{9-\delta}$ as a function of oxygen content $9-\delta$ and of the La for Ba substitution in at–%.

$T_c$ of $Y(Ba_{1-y}La_y)_2Cu_3O_{9-\delta}$ increases with increasing oxygen content up to the lower limit of $\delta$, where the Cu valency reaches ~2.30. This happens irrespectively whether or not the oxygen content exceeds $9-\delta = 7$. $T_c$ decreases nonlinearly with increasing La/Ba substitution. The nonlinearity is assumed [6] to be a consequence of a redistribution of oxygens in the Cu—O chains, leading to a transition from the orthorhombic to tetragonal crystal structure. As a consequence of both Sr and La substitutions, an anisotropic compression of the structure takes place along the $c$ axis. The degree of compression correlates with the decrease of $T_c$, as long as the Cu valency is kept constant (i.e., the formal average concentration of hole carriers is constant).

### 4.3. Cu–substituted $YBa_2Cu_3O_{9-\delta}$

Generally, upon any substitution for Cu in $YBa_2(Cu_{1-z}M_z)_3O_{9-\delta}$, a decrease in $T_c$ is observed. Phenomenologically, the substituents may be divided into three groups according to their effect on $T_c$:

($\mathcal{A}$) Substituents causing an initially rapid decrease of $T_c$. Zn and Mg may serve here as examples, with $(\partial T_c/\partial z)_{z=0.005} \cong -1200$ K.

($\mathcal{B}$) Substituents causing a tilde–shaped ($\sim$) decrease of $T_c$, with an induction period and an intermediate value of the substitutional derivative at the maximal decrease. Fe and Co with maximum $(\partial T_c/\partial z) \cong -800$ K at the inflexion point ($z \cong 0.05$) exemplify this case.

($\mathcal{C}$) Substituents with an almost linear decrease of $T_c$ and with low substitutional derivative. As examples, Ni with $(\partial T_c/\partial z)_{z=0.005} \cong -400$ K and Li with $(\partial T_c/\partial z)_{z=0.03} \cong -200$ K.

## 4.4. Correlation of $T_c$ with Structural Characteristics

Any correlation between the observed differences in behaviour of the substituted phases and the fundamental properties of the solid are of obvious interest in order to abstract the preconditions of the high-$T_c$ superconductivity and to test the theoretical hypotheses. Generally, $T_c$ should be correlated to variables in terms of electronic wave functions represented in the band structure of the solid. However, since these primary variables are not accessible for comparison, a correlation is sought to the derived properties, e.g., crystallochemical variables, like Cu coordination, Cu—O bond distances, short range order of the oxygen vacancies, and roughly also to the unit cell metric. Naturally, the important transport properties, like the concentration of charge carriers, should be considered as well.

To discuss the suppression of $T_c$ in connection with structural changes, two principal structural distortions may be introduced, which both have been used in formulating phenomenological rules on occurence of superconductivity in the 123 phase:

(1) The *orthorhombic distortion*, $D_{b/a} = (b/a) - 1$, which to some extent may serve as a gauge for the continuity of the Cu—O chains;

(2) The *tetragonal deformation*, $D_{c/ab} = [2c/3(a+b)] - 1$, which narrows the band at the Fermi level, or, in a ligand field model, forms a more solitary, partially filled orbital.

An overview showing $T_c$ and the tetragonal deformation for the particular substituents in $YBa_2Cu_3O_{9-\delta}$ is given in Fig. 9.

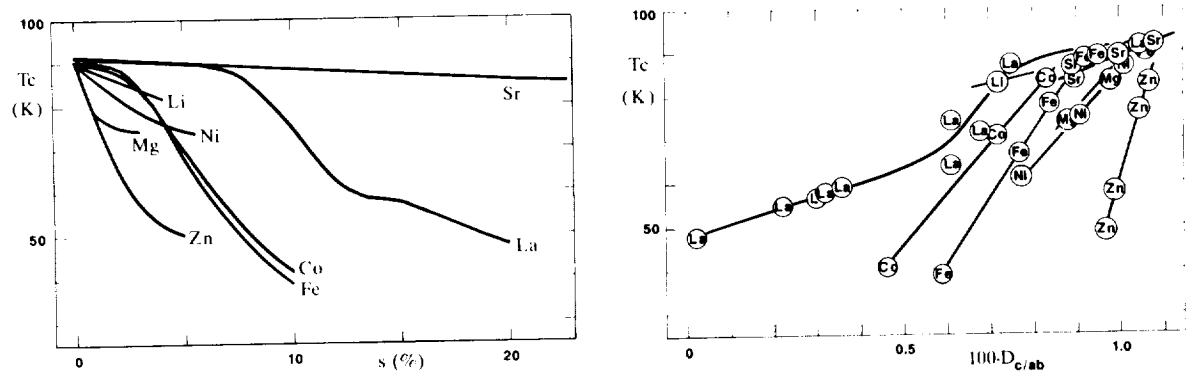


**Figure 9.** $T_c$ of substituted, oxygen-saturated $YBa_2Cu_3O_{9-\delta}$ (substitution $s$ in %) and the tetragonal deformation $D_{c/ab} = [2c/3(a+b)] - 1$.

No change in $T_c$ is observed upon varying the effective size of an equivalent atom at the Y-site (substitution by RE), which separates the Cu—O slabs in the structure. A contraction of the Cu—O slabs upon substitution of the large Ba by the smaller Sr atom is accompanied by a mild suppression of $T_c$, whereas the La/Ba substitution decreases $T_c$ more strongly. A significant decrease in $T_c$ is observed with substitutions for Cu. Of these, the most effective suppressors of $T_c$, *viz.*, Zn and Mg do not decrease the orthorhombic distortion of the structure. The Fe and Co substituents, which rapidly induce the tetragonal structure (by PXD), are rather mild suppressors of $T_c$, and superconductivity is maintained in the tetragonal phase over a wide substitutional range. However, a possible effect of the short range vacancy ordering in the twinned orthorhombic nanodomains [31] may be considered, which would preserve a certain length of the Cu—O chains even within the apparent tetragonal symmetry. The substitution by Li appears to suppress $T_c$ the least, though a significant decrease in the orthorhombic distortion is observed.

On the other hand, a decrease in the tetragonal deformation is always accompanied by a decrease of $T_c$ for all substitutions, see Fig. 9. If the substituents are correlated to $T_c$ according to the extent of the tetragonal deformation, Sr, La and Li emerge in one group with Fe and Co (which substitute for Cu in the chains) in another group. The strongest suppression of $T_c$ is provided by

Ni, Mg and Zn, which replace the Cu atoms having square–pyramidal coordination. Zn acts most effectively, possibly by introducing a portion of the $d^{10}$ state at the Cu–site, thereby decreasing the hole concentration.

The experiments on substitution seem to support the view that the Cu—O pyramidal sheets are crucial for the superconductivity in cuprates, where they apparently serve as pairing centres. As such, they are very sensitive to any alteration of the local electronic structure and to deformations which would degenerate the Cu $(3d_{x^2-y^2})$—O $(2p_{x,y})$ orbitals participating in the band at the Fermi level. The Cu—O chains, serving then as charge reservoirs, are less capable of destroying superconductivity. A rather massive alteration of the local electronic structure, a large charge deficit or a considerable structural disorder must be introduced in the chains in order to suppress the superconductivity.

**Acknowledgement** This work has received financial support from the Norwegian Council for Science and Humanities (NAVF). The assistence of Cand. mag. Rita Glenne and Cand. scient. Per H. Andresen in some experiments is gratefully acknowledged.

## References

1. Karen, P., Braaten, O., Fjellvåg, H. and Kjekshus, A. *Acta Chem. Scand.* **44** (1990) (submitted).
2. Andresen, A. F., Fjellvåg, H., Karen, P. and Kjekshus, A. *Z. Cryst. 185* (1988) A2.
3. Karen, P., Fjellvåg, H., Kjekshus, A. and Andresen, A. F. *J. Solid State Chem.* (submitted).
4. Karen, P., Andresen, P. H., Fjellvåg, H. and Kjekshus, A. *Acta Chem. Scand.* **44** (1990) (submitted).
5. Fjellvåg, H., Karen, P., Kjekshus, A. and Andresen, A. F. *Physica C (Amsterdam)* **162–164** (1989) 49.
6. Karen, P., Fjellvåg, H. and Kjekshus, A. *Supercond. Sci. Technol.* **3** (1990) (submitted).
7. Frase, C. G. , Liniger, E. G. and Clarke, D. R. *J. Amer. Ceram. Soc.* **70**[9] (1987) C–204.
8. Roth, R. S., Davis, K. L. and Dennis, J. R. *Adv. Ceram. Mat.* **2**[3B] (1987) 303.
9. Wang, G., Hwu, S.-J., Song, S. N. , Ketterson, J. B. , Marks, L. D. , Poeppelmeier, R. and Mason, T. O. *Adv. Ceram. Mat.* **2**[3B] (1987) 313.
10. Fjellvåg, H., Karen, P. and Kjekshus, A. *Acta Chem. Scand. A* **41** (1987) 283.
11. DeLeeuw, D. M., Mutsaers, C. A. H. A. , Geelen, G. P. J. , Smoorenburg, H. C. A. and Langereis, C. *Physica C (Amsterdam)* **152** (1988) 508.
12. Ahn, B. T., Lee, V. Y., Beyers, R., Gür, T. M. and Huggins R. A. *Physica C (Amsterdam)* **162–164** (1989) 883.
13. Borowiec, K. and Kolbrecka, K. *Jpn. J. Appl. Phys.* **28** (1989) L1963.
14. Fjellvåg, H., Karen, P., Kjekshus, A., Kofstad, P. and Norby, T. *Acta Chem. Scand. A* **42** (1988) 178.
15. Arjomand, M. and Machin, D. J. *J. Chem. Soc. Dalton Trans.* **1975** 1061.
16. Webb, A. W., Skelton, E. F., Qadri S. B., Carpenter E. R., Osofsky, M. S., Jr., Soulen, R. J. and Le Tourneau, V. *Physica C (Amsterdam)* **162–164** (1989) 899.
17. Karpinski, J. and Kaldis, E. *Nature* **332** (1988) 242.
18. Sato, M., Konaka, T. and Sankawa, I. *Jpn. J. Appl. Phys.* **27** (1988) L1047.
19. Dai, Y., Manthiram, A., Campion, A. and Goodenough, J. B. *Phys. Rev. B: Condens. Matter* **38** (1988) 5091.
20. Rao, C. N. R. , Ganguly, P., Hedge, M. S. and Sarma, D. D. *J. Amer. Chem. Soc.* **109** (1987) 6893.
21. Karpinski, J., Rusiecki, S., Bucher, B., Kaldis, E. and Jilek, E. *Physica C (Amsterdam)* **161** (1989) 618.
22. Nevřiva, M., Pollert, E., Šesták, J. and Třiska, A. *Thermochimica Acta* **127** (1988) 395.
23. Fjellvåg, H., Karen, P., Kjekshus, A. and Grepstad, J. K. *Acta Chem. Scand. A* **42** (1988) 171.
24. Osamura, K. and Zhang, W. *Jpn. J. Appl. Phys.* **26** (1987) L2094.
25. De Leeuw, D. M., Mutsaers, C. A. H. A., Langereis, C., Smoorenburg, H. C. A. and Rommers, P. J. *Physica C (Amsterdam)* **152** (1988) 39.
26. Ruddlesden, S. N. and Popper, P. *Acta Crystallogr.* **11** (1958) 54.
27. Tokura, Y., Takagi, H., Uchida, S. *Nature* **337** (1989) 345.
28. McCarron, E. M. , Subramanian, M. A. , Calabrese, J. C. and Harlow, R. L. *Mater. Res. Bull.* **23** (1988) 1355.
29. Fjellvåg, H., Karen, P., Kjekshus, A. and Andresen, A. F. *Physica C (Amsterdam)* **162–164** (1989) 49.
30. Karen, P., Fjellvåg, H., Kjekshus, A. and Andresen A. F. *J. Solid State Chem.* (submitted).
31. Hiroi, Z., Takano, M., Takeda, Y., Kanno, R., and Bando, Y. *Jpn. J. Appl. Phys., Part 2* **27** (1988) L580.